

“half-electron ($e/2$)” - free electron fractional charge induced by twisted light

Yiming Pan^{1*}, Ruoyu Yin^{2*}, Yongcheng Ding³, Daniel Podolsky⁴, Bin Zhang^{1,5}

1. School of Physical Science and Technology and Center for Transformative Science, ShanghaiTech University, Shanghai 200031, China
2. Department of Physics, Institute of Nanotechnology and Advanced Materials, Bar-Ilan University, Ramat-Gan 52900, Israel
3. Department of Physical Chemistry, University of the Basque Country UPV/EHU, Apartado 644, 48080 Bilbao, Spain
4. Department of Physics, Technion, Haifa 3200003, Israel
5. Department of Electrical Engineering Physical Electronics, Tel Aviv University, Ramat Aviv 6997801, Israel

Abstract

Recent advances in ultrafast electron emission, microscopy, and diffraction reveal our capacity to manipulate free electrons with remarkable quantum coherence using light beams. Here, we present a framework for exploring free electron fractional charge in ultrafast electron-light interactions. An explicit Jackiw-Rebbi solution of free electron is constructed by a spatiotemporally-twisted laser field, showcasing a flying topological quantum number with a fractional charge of $e/2$ (we call it “half-electron”), which is dispersion-free due to its topological nature. We also propose an Aharonov-Bohm interferometry for detecting these half-electrons. The half-electron is a topologically protected bound state in free-space propagation, expands its realm beyond quasiparticles with fractional charges in materials, enabling to advance our understanding of exotic quantum and topological effects of free electron wavefunction.

Modern physics permits fractional charges. There are two approaches to pursue such an exotic existence. One method examines the topological structure of the massive Dirac equation, firstly demonstrated by the Jackiw-Rebbi solutions in quantum field theory [1]. The other delves into many-body interactions in condensed matters, exemplified by the Laughlin's wave function in Fractional Quantum Hall Effect (FQHE) [2]. Both realizations are in need of materials such as polyacetylene [3], semiconductors [4], and artificial disclinations [5–8]. Traditionally, electrodynamics assume that electrons carry only integer electric charges, with no allowance for fractional charges. However, in 1976, Jackiw and Rebbi challenged this conventional wisdom by proposing the existence of zero-energy modes that emerge from the Dirac equation upon the introduction of a mass term with a kink profile. They argued that these zero modes carry fractional charges, specifically $e/2$ [1]. Su, Schrieffer, and Heeger's seminal discovery in Polyacetylene in 1979 [3] confirmed this prediction. Further evidence has been provided by the FQHE [9], in which quasiparticles clearly exhibited fractional charges. Numerous proposals and experimental investigations are actively exploring elusive fractional charges, with a particular focus on quantum materials [10,11], topological photonics with disclinations [12,13]. Yet, the detection of fractional charge remains slightly indirect such as LDOS, shot noise measurement, edge state current, Aharonov-Bohm oscillations [4,14–18], and direct use of fractional charge is even far from being feasible. These fascinating avenues raise a question: Is it possible to construct material-free particle carrying fractional charge, and if so, can we measure the flying fractional charge in free space?

It is worth noting that our proposal of free electron fractional charge aligns well with the developing frontier of attosecond physics. Recent advances in ultrafast free electrons have revolutionized electron microscopy [19], diffraction [20], and free electron radiation and lasing [21,22]. Electron beams have obtained extremely high resolution in femtoseconds and attoseconds [23–25]. However, there is a challenge to overcome: the inevitable dispersion and propagation chirping of ultrashort electron pulses, even in vacuum. For example, a slow electron, operating at energies of 100 eV, is not immune to the nonrelativistic dispersion. Understanding and controlling the dispersion effect of slow electrons is crucial for harnessing and characterizing attosecond electron pulses in innovative experiments, as recently demonstrated by [26–29]. Therefore, the field of electron wavefunction quantum engineering presents enormous potential, offering a deeper understanding of the quantum realm and opening doors to groundbreaking technological advances [29–32]. Turning to the prospect of generating and detecting fractional charges in free space, our focus now shifts to recent low-

energy electron optics with several hundred electronvolts. These advancements have unveiled the fascinating effects of dispersion during low-energy interactions, such as free electron Rabi oscillations [33–35], which are crucial in our pursuit.

Here, we present a pioneering strategy that exploits the dispersion of wide spectral sidebands to construct an effective interaction of a pulsed “two-level” electron (only two sidebands involved, see Fig. 1b) [33]. This Dirac-type interaction arises from the coupling of electrons with a laser beam that is spatiotemporally twisted, successfully imitating the kink profile of the mass term in the celebrated Jackiw-Rebbi model [1]. The resulting light-induced domain wall inherits a topological quantum number, yielding a fractional charge of $e/2$, which we refer to as “half-electron.” This half-electron propagates in a topological dispersion-free manner, a striking property for the manipulation of slow-electron wavefunctions. To validate and detect the half-electron, we further propose an experiment of Aharonov-Bohm interferometry that enables to demonstrate the period- 4π oscillation in the interference pattern of the photocurrent measurement.

Constructing slow-electron Dirac equation by light. The nonrelativistic low-energy electron Hamiltonian in the presence of electromagnetic field is given by $H = \frac{(\mathbf{p}-e\mathbf{A})^2}{2m}$. We assume the longitudinal vector potential and the electric field are modulated by a grating, given by $A = \frac{E_0}{\omega} \cos[\omega t - qz - \theta(z, t)]$, and $E = -\frac{\partial A}{\partial t} = E_0 \sin[\omega t - qz - \theta(z, t)]$, respectively, where ω is the frequency, q is the wavevector, and $\theta(z, t)$ is the initial phase. A spatiotemporally-varying kink profile would be imprinted on this phase term, which we will discuss it later. Note that we assume that the vector potential, as well as the electric field, is along the traveling direction of the electron, z direction.

Such modulation of electrons by electromagnetic fields, or essentially electron-photon interactions, described by Eq. (1), can be classified through the Raman-Nath and Bragg regimes, each distinguished by distinct phase matching conditions and coupled-mode equations [33,34]. In Raman-Nath regime, characterized by weak-field coupling, the phase matching condition ensures efficient interaction when the electron's wavevector aligns with that of incoming photons, leading to multiphoton scattering events and phase accumulation, as shown in Fig. 1a. Conversely, the Bragg regime entails strong-field interactions, with a modified phase matching condition accounting for the periodicity of the synthetic lattice [33]. Electrons undergo Bragg diffraction in synthetic dimension, and their momentum is quantized by light, offering precise

control and manipulation. Coupled-mode equations that are vital for our discussions, in Bragg regime under investigation in this Letter, are simplified in the momentum representation, and in the co-moving frame ($z \rightarrow z - \omega t/q$) as

$$\begin{aligned} i\hbar \partial_t |\delta k - q/2\rangle &= \left[\frac{\hbar^2 \delta k^2}{2m} - \left(\frac{\hbar^2 q}{2m} \right) \delta k \right] |\delta k - \frac{q}{2}\rangle - \kappa^* |\delta k + \frac{q}{2}\rangle \\ i\hbar \partial_t |\delta k + q/2\rangle &= \left[\frac{\hbar^2 \delta k^2}{2m} + \left(\frac{\hbar^2 q}{2m} \right) \delta k \right] |\delta k + \frac{q}{2}\rangle - \kappa |\delta k - \frac{q}{2}\rangle \end{aligned} \quad (1)$$

Here the coupling coefficient $\kappa = \frac{eE_0 \hbar k}{2m\omega} e^{i\theta(z,t)}$, depending on the amplitude strength E_0 and the spatiotemporally-varying phase profile $\theta(z,t)$. Since the momentum k is a continuous number, we fix $k = k_0 + \delta k$, and also shift $\delta k \rightarrow \delta k \pm q/2$. We assume the condition $\frac{\hbar^2 (q/2)^2}{2m} \gg |\kappa|$, namely using the approach of adiabatic elimination [36] to truncate the coupled modes into the case involving two sidebands [34]. See Methods for more details of the truncation. Defining the wavefunction as a spinor $|\tilde{\psi}\rangle = \alpha |\delta k - \frac{q}{2}\rangle + \beta |\delta k + \frac{q}{2}\rangle = [\alpha, \beta]^T$, Eq. (2) can be rewritten as

$$i\hbar \partial_t |\tilde{\psi}\rangle = \frac{\hbar^2 \delta k^2}{2m} |\tilde{\psi}\rangle - \frac{\hbar^2 q}{2m} \delta k \cdot \sigma_z |\tilde{\psi}\rangle - |\kappa| e^{-i\theta} \sigma_z \sigma_x |\tilde{\psi}\rangle \quad (2)$$

Correspondingly, the effective Dirac Hamiltonian is constructed as

$$H_D = \frac{\hbar^2 \delta k^2}{2m} \sigma_0 - \frac{\hbar^2 q}{2m} \delta k \cdot \sigma_z - |\kappa| e^{-i\theta} \sigma_z \sigma_x \quad (3)$$

where σ_0 is an identity matrix, σ_z and σ_x are the Pauli- z and Pauli- x matrices. Notice that the first term is a dispersion term, it is negligible in the approximation $\delta k \ll q$. For the case of a constant phase θ , we can easily obtain the Dirac dispersion $E_{\pm} = \pm \sqrt{\left(\frac{\hbar^2 q}{2m} \delta k \right)^2 + |\kappa|^2}$, see the inset of Fig. 1a.

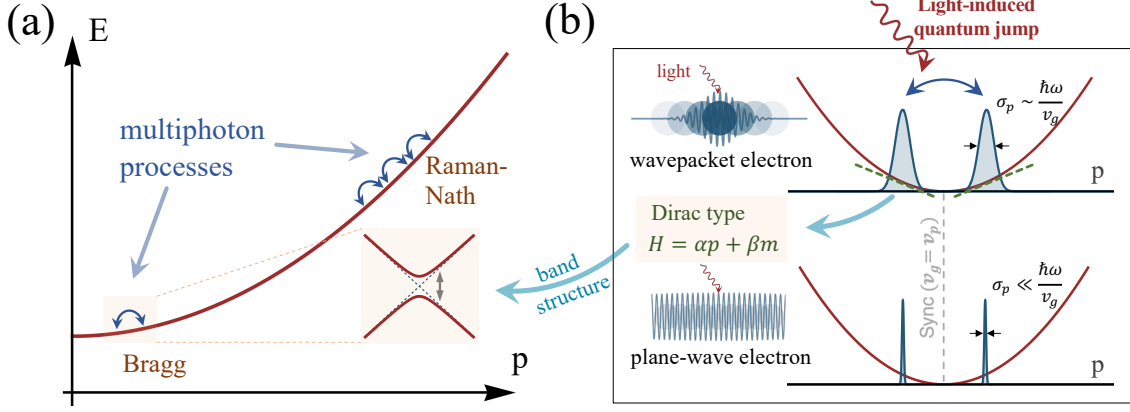


Fig. 1: (a) Multiphoton processes represented on the energy dispersion, and for the slow (fast) electron interaction, Bragg (Raman-Nath) diffraction occur. In Bragg regime (orange region), where only two sidebands involved, we construct the effective Dirac-type equation of the “two-level” free electron. Specifically, as seen in (b), the energy spread of the point-like electron plays the momentum term of the Dirac equation, while the light-electron coupling strength plays the Dirac mass term.

Free electron Jackiw-Rebbi solutions. We consider a simple Dirac mass term with a kink structure, the wavefront profile of the laser as shown in Fig. 2b,

$$\kappa(z, t) = \kappa\left(z - \frac{\omega t}{q}\right) = |\kappa| e^{-i\theta(z - \omega t/q)\sigma_z} = \begin{cases} +|\kappa|, & \text{for } z - \omega t/q = -\infty \\ -|\kappa|, & \text{for } z - \omega t/q = +\infty \end{cases} \quad (4)$$

allows to calculate the zero-mode solution ($i\hbar\partial_t\psi_0 = 0$)

$$\left(-\frac{\hbar^2 q}{2m} \delta k \cdot \sigma_z - |\kappa| e^{-i\theta\sigma_z} \sigma_x\right) \psi_0 = 0 \quad (5)$$

We neglect the first quadratic term in Eq. (4) and recall the spatial representation,

$$\left[-i\frac{\hbar^2 q}{2m} \sigma_z \partial_z + \kappa(z)\sigma_x\right] \psi_0 = 0 \quad (6)$$

Multiplying both sides of Eq. (7) from the left with σ_z yields $\left[-i\frac{\hbar^2 q}{2m} \partial_z + i\kappa(z)\sigma_y\right] \psi_0 = 0$.

Hence, we write the zero-mode solution as $\psi_0(z) = \chi_{\pm}^{(y)} \varphi_{\pm}(z) = \frac{1}{\sqrt{2}} \begin{bmatrix} 1 \\ \pm i \end{bmatrix} \varphi_{\pm}(z)$, with $\varphi_{\pm}(z)$

determined by $\frac{\hbar^2 q}{2m} \partial_z \varphi_{\pm}(z) = \pm \kappa(z) \varphi_{\pm}(z)$. Therefore, we obtain an explicit JR solution of

free electron, as given by $\psi_0^{(\pm)} = \frac{1}{\sqrt{2}} \begin{bmatrix} 1 \\ \pm i \end{bmatrix} \text{Exp} \left[\pm \frac{2m}{\hbar^2 q} \int_0^z \kappa(\xi') d\xi' \right]$. Since one of the solutions

diverges exponentially ($\psi_0^{(-)}$) due to kink profile (Eq. (5)), we abandon this unphysical solution that cannot be normalized. Only one solution with a special chirality ($\psi_0^{(+)}$) remains. Roughly speaking, this chiral zero mode would lead to half-electron ($e/2$), which will be expound in the next section. Return to the original representation of the time dependent Schrodinger equation, we express the full free electron Jackiw-Rebbi solution as

$$\psi_0(z, t) = \left(\frac{e^{-i(qz-\omega t)/2} + i e^{i(qz+\omega t)/2}}{\sqrt{2}} \right) e^{ik_0 z - i \left(\frac{\hbar q^2}{8m} \right) t} e^{\frac{2m}{\hbar^2 q} \int_0^{z-\omega t/q} |\kappa(\xi')| d\xi'} \quad (7)$$

To achieve and implement the half-electron solution, we employ the laser whose phase profile is modulated by a Spatial Light Modulator (SLM). As illustrated in Fig. 2, the femtosecond laser beam is split into two, one of which to stimulate the photocathode to emit electrons, following a Second Harmonic Generation (SHG) by generating UV light. The other beam is modulated by the SLM to form homogeneous or twisted wavefront of the coupling laser field. Light gratings (the colored blocks with squared wave inside) are utilized to guarantee the phase matching condition during interactions. In (a), an electron remains as a carrier of one unit of charge, under the homogeneous wavefront, showing dispersive. While if we use a precisely-controlled rotating SLM to twist the beam wavefront, there will be a solitary wave carrying topological charge of $e/2$ (from the viewpoint of topological insulator [37]) “surfing” on the kink structure of the twisted wavefront. We choose the comoving kink profile as $\kappa(\xi) = -|\kappa| \tanh(\xi)$, the profile of the solitary solution would be proportional the sech $(z - \omega t/q)$, exhibiting light-induced non-spreading feature (also see Eq. (A1) in the Methods).

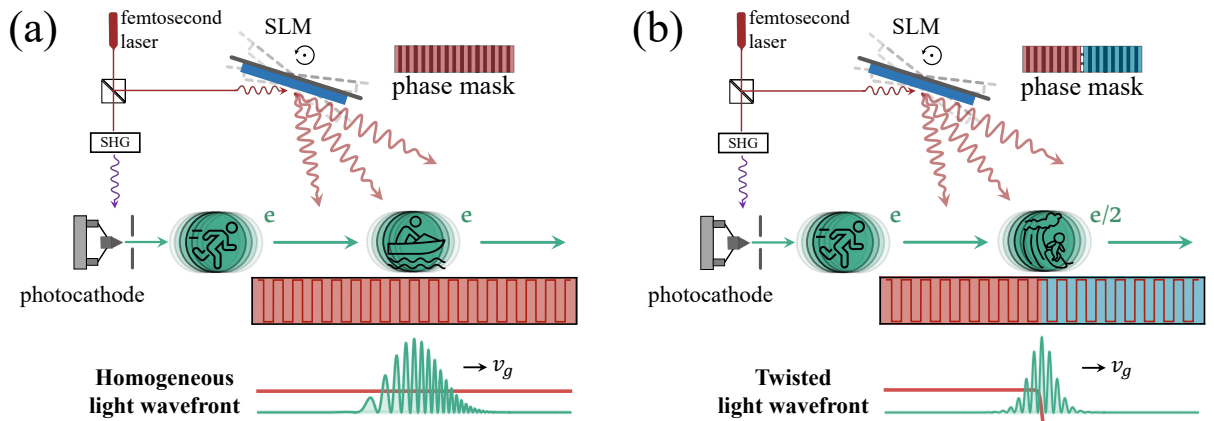


Fig.2: The schematic setup of the interaction of (a) one-electron (with charge of e) or (b) half-electron (carrying $e/2$) with a homogeneous or spatiotemporally twisted laser beam.

Simulation of the temporal profile of $e/2$. Fig. 3 gives a direct simulation of the half-electron, using the time-dependent Schrodinger equation in the presence of the twisted light wavefront. An electron wavepacket, profiled as a Gaussian in the momentum space, featuring a center energy of 100 eV ($\beta = v_0/c = 0.02$), is manipulated such that the dispersion from the center energy is larger than the laser photon energy ($\lambda = 200$ nm and $\hbar\omega = 6.2$ eV). Subsequently, the electron traverses a grating structure designed to synchronize the light-induced near field with the electron, specifically $\omega/q = v_0$. Crucially, the center of the electron wavepacket undergoes fine-tuning to align with the center of the twisting structure of the laser wavefront. For the latter we chose a specific twisted phase profile $\theta(z, t) = \frac{\pi}{2} \tanh\left(\frac{z-v_0t}{0.001}\right)$ to achieving the flying kink. The near field interacts in the grating structure with the electron, through the minimal coupling $A \cdot p$ in the time-dependent Hamiltonian. The evolving electron wavefunction in space and with time is recorded and plotted in Fig. 3. Notably, when comoving with the electron's wave center, the soliton profile becomes evident (Eq. 7), and the dispersion-free property, a consequence of topological protection, is illustrated in the inset of Fig. 3. The "bound state" imposes self-constraints over time. For additional details regarding the simulation algorithm, see Supplementary Information.

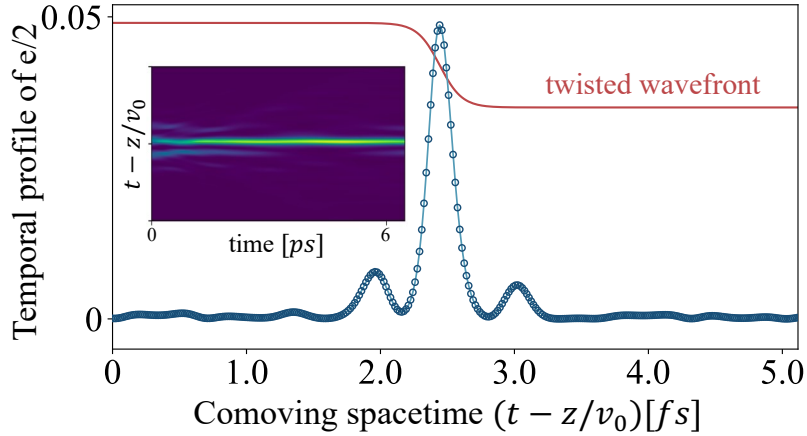


Fig. 3: TDSE simulation of temporal profile of “half-electron ($e/2$)” by a twisted light wavefront. The induced half-electron spatiotemporal profile is clearly pinned at the light-induced kink structure generated by the twisted light wavefront (red curve). The temporal profile is spanned with a duration of 5 femtosecond in our simulation. The inset figure presents a dispersion-free temporal profile of the half-electron after evolving with time from 0 to 6 ps, indicating a protection of its topological nature of $e/2$. The simulation parameters are given in the main text.

“Half electron” with fractional charge of $e/2$. As later we will prove from quantum field theory, this is a twisted light induced electron state that carries a fractional charge, due to topological protection. Now we want to tune the phase of the light wavefront $\theta(z, t)$ to show the fractional charge of the zero-energy solution (Eq. 9). To apply the Goldstone-Wilczek formula [38], we rewrite the effective Dirac Hamiltonian H_D in the field-quantization formulation

$$\tilde{H}_D = \int dz \Psi^\dagger(z) \left(\frac{\hbar^2 \delta k^2}{2m} \mathbb{1}_2 - \frac{\hbar^2 q}{2m} \delta k \cdot \sigma_z - |\kappa| e^{-i\theta \sigma_z} \sigma_x \right) \Psi(z) \quad (8)$$

where the electron field operator $\Psi(z)$ is for second quantization. We can directly apply the Goldstone-Wilczek formula [38], and obtain the 2-current $J^\mu = (\rho, \mathbf{j}_z) = \frac{e}{2\pi} \epsilon^{\mu\nu} \partial_\nu \theta$. Hence, the transferred charge ΔQ for a spatiotemporally varying phase, $\theta(z, t)$, is determined by

$$\Delta Q = -\frac{e}{2\pi} \int dz \partial_z \theta(z) = -\frac{e}{2} \quad (9)$$

This essentially indicates that tuning the phase of the light beam, which interacts with electrons under synchronization condition, will drive the gauge anomaly and a fractional charge. Specifically, an anti-kinked domain wall of θ carries a half-charge $\pm e/2$, with the sign determined by the sign of the difference between boundary values, $\theta(+\infty) - \theta(-\infty)$.

The nature of half-electron is far from being a mere combo of a kink and a fermion, which is a common misconception. Instead, the half-electron is fundamentally constituted by the interplay between the electromagnetic fields and free electron, resembling the topological soliton that interplay between photons and Bloch electron in polyacetylene. The half-electron, considered a topological defect, emerges as an entity composed from both bosonic condensation and Dirac-type fermionic fields. In Jackiw’s original viewpoint [1], there exist two states for the kink: one with filled zero mode (half-electron) and the second with zero mode empty (half-hole) [39]. The half-hole is reasonably when the system is filled up to a Fermi level at the energy gap. However, for free electrons, there is no concept of “Fermi level”. We suggest interpreting the presence of half-hole is equal to the half-electron in free space due to the topological nature ($-\pi \rightarrow \pi - (2\pi)$), in this sense that an electron is split into two pieces by a twisted laser. Therefore, our proposal that splits one electron into two half-electrons, is a pivotal concept revolving around the generation and annihilation of free electron kink-antikink pairs, with each kink contributing an increment of $e/2$ to the overall charge of an electron.

Experimental verification. To verify the fractional charge, there are few approaches have been experimentally tested in solids, such as the shot-noise experiment [40] and the Mach-Zehnder interferometer (MZI) with Aharonov-Bohm (AB) oscillations [41,42]. Therefore, we suggest a possible experimental setup for free electron fractional charge as presented in Fig. 4. The MZI setup is using the AB effect to measure the quantum interference pattern of the fractional charge: $\exp(-i \frac{q\Phi}{\hbar c})$, with $q = e/2$ for a half-electron, $q = e$ for a conventional electron, respectively. Notice that electron's spin degeneracy can be polarized by selecting with an inhomogeneous magnetic field, such as the polarized electron source technology for transmission electron microscopy [43].

We then introduce a light grating to facilitate light-electron interactions, ensuring phase-matching conditions. By utilizing a spatial light modulator (SLM), we tailor the light to manifest a flying “kink” structure in its phase, as posited in our theoretical framework. Under this light modulation, the incident electron exhibits a solitary solution bearing a charge of $e/2$, as illustrated in Fig. 2. Subsequently, the electron beam splits, traveling around a hole dug within the grating. An external magnetic flux penetrates this hole, imparting a phase difference to the bifurcated electron beam via the Aharonov-Bohm effect. At the hole's antipodal point relative to the electron's split, we facilitate interference between the beams. Detection of the resulting current is achieved using a microchannel plate (MCP) detector and a CCP camera. Note that the MCP detector should be practically shielded by an optical filter in order to suppress its unwanted response to the optical field on the nanograting. The photocurrent oscillation that stems from the interference of wavefunctions varies with the magnetic flux. Given that the post-encirclement phase relative to the magnetic flux is $-q\Phi/\hbar c$, the charge q delineates the current's periodicity as a function of magnetic flux Φ . Our predictions suggest that the half-electron with $e/2$ will yield a current 4π -oscillation, with a period twice that of an electron, the latter being ascertainable by turning on/off the laser. This method offers a possible experimental approach to validate the existence of light-induced half-electron.

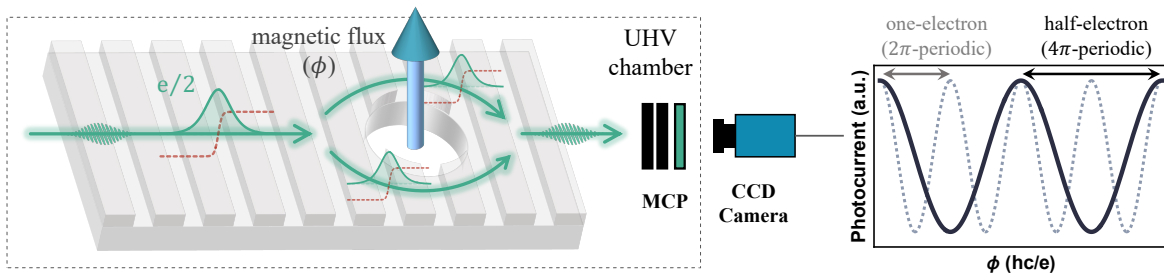


Fig. 4: A proposal of free electron Aharonov-Bohm (AB) interferometry to detect “half-electron ($e/2$)”. (a) We use a light grating with a hole to allow phase matching between the laser beam and electron. The half-electron wavefunction is split into two beams surrounding an external magnetic flux (ϕ) piercing the grating hole, then they recombine to generate oscillating photocurrents collected by a MCP detector. (b) The photocurrent from the AB interferometry in terms of the magnetic flux ϕ . When the laser is turned on (or off), due to the electron beam carries half (or one unit of charge), leading to the 4π -period (or 2π -period) of photocurrent oscillation.

To this point, our study enables to pave the way for advancing quantum simulations using free electrons, capitalizing on their inherent 'clean quantumness'. Free electrons, a fundamental object since the inception of quantum mechanics, exhibit manipulatable coherence and intrinsic inclination to interact with photons, allowing for fine tuning to engineer their energy levels, e.g., our zero-mode creation in the light-induced Dirac-type band structure. Echoing the work in Ref. [44], our findings indicate that manipulating quantum light interacting with electrons, as specifically proposed in the work, can profoundly shape the latter. In essence, information transfer between light and electrons within a photon-electron-entangled system becomes feasible [45]. Our discovery, particularly the creation of the half-electron through the light wavefront's twisting and its influence on the mass term in the constructed Dirac equation, signifies a brand-new method for quantum simulations [46–50]. This approach, centered on designing light to modulate electrons, could revolutionize our understanding and manipulation of exotic quantum systems.

Conclusions and outlook. In this work, we have constructed the Jackiw-Rebbi solution for free electrons using a spatiotemporally-twisted laser field, leading to the discovery of a novel fractional charge of $e/2$, “half-electron”. This free electron fractional charge is a quantum number having topological nature. Our work elucidates the emergence of fractional charges in vacuum rather in material. Notably, half electron remains spatiotemporally localized, a prominent feature for manipulating electron wavefunctions in low-energy electron quantum optics. Our construction of light-induced half-electron has profound implications, extending the domain of exotic fractional charges beyond conventional realms of materials and nanofabrication, suggesting that such entities can be facilitated as a novel electron source for microscopy and spectroscopy.

Added that to validate this groundbreaking concept and achieve a tangible detection of the half-electron, we advocate for the free electron Aharonov-Bohm interferometry. The proposed experiment exploits a 4π -period of the interference pattern, a signature that distinctly contrasts the conventional 2π -period. Collectively, our findings offer a promising pathway for exploring and harnessing exotic quantum effects in ultrafast electron optics and quantum wavefunction engineering.

Importantly, our research suggests a promising paradigm shift to study the physics of free electron topological phases, leveraging the unique advantages of material-free. By employing light beams to simulate or mimic lattice structures—a technique akin to what is achieved in photon-induced near-field electron microscopy (PINEM) [19]—we open new vistas in studying phenomena traditionally reserved for condensed-matter physics within free photon-electron-coupling systems. This novel approach allows for the light-modulated electrons to emulate electrons in solids, yet they are trapped not by atomic potentials but by light fields. Consequently, atomic potential typical in materials can be analogously achieved through optical tuning. The fundamental dynamics of these systems, as revealed by our current work, demonstrate that Dirac-type equations and hopping phenomena induced by light, can be harnessed to replicate linear band structures seen in graphene, Weyl semimetal, and topological materials, now within a free electron-light framework. This work may have added one more brick to the developing free-electron condensed matter physics in compliment with the free electron synthetic dimensions. Further exploration of free electrons with space-charge interactions [51,52], which is absent in this work, warrants attention, as it will unlock additional possibilities for emulating many fantastic physics such as strongly-correlated systems.

Acknowledgements

We thank Huaiqiang Wang, Dandan Hui for insightful discussions. Y.P. is supported by the National Natural Science Foundation of China (Grant No. 2023X0201-417). R.Y. is supported by the Israel Science Foundation's grant 1614/21.

The authors declare no competing financial interests.

Correspondence and requests for materials should be addressed to Y.P.

(yiming.pan@shanghaitech.edu.cn), R.Y.(yinruoy@biu.ac.il)

References

- [1] R. Jackiw and C. Rebbi, Phys. Rev. D **13**, 3398 (1976).
- [2] R. B. Laughlin, Phys. Rev. Lett. **50**, 1395 (1983).
- [3] W. P. Su, J. R. Schrieffer, and A. J. Heeger, Phys. Rev. Lett. **42**, 1698 (1979).
- [4] X.-L. Qi, T. L. Hughes, and S. Zhang, Nat. Phys. **4**, 273 (2007).
- [5] C. W. Peterson *et al.*, Nature 2021 589:7842 **589**, 376 (2021).
- [6] Y. Liu *et al.*, Nature **589**, 381 (2021).
- [7] G. Van Miert and C. Ortix, Phys. Rev. B **97**, 201111 (2018).
- [8] T. Li *et al.*, Phys. Rev. B **101**, 115115 (2020).
- [9] H. L. Stormer, D. C. Tsui, and A. C. Gossard, Rev. Mod. Phys. **71**, S298 (1999).
- [10] J. Orenstein, Phys Today **65**, 44 (2012).
- [11] Y. Tokura, M. Kawasaki, and N. Nagaosa, Nat. Phys **13**, 1056 (2017).
- [12] B. Ren *et al.*, APL Photonics **8**, 16101 (2023).
- [13] B. Ren *et al.*, Light Sci Appl **12**, 194 (2023).
- [14] C. Beenakker and C. Schönberger, Phys Today **56**, 37 (2003).
- [15] R. L. Willett, L. N. Pfeiffer, and K. W. West, Proceedings of the National Academy of Sciences **106**, 8853 (2009).
- [16] S. C. Morampudi *et al.*, Phys. Rev. Lett. **118**, 227201 (2017).
- [17] Z. c ć *et al.*, Phys. Rev. X **8**, 11037 (2018).
- [18] J. Nakamura *et al.*, Nat. Phys. **16**, 931 (2020).
- [19] B. Barwick, D. J. Flannigan, and A. H. Zewail, Nature **462**, 902 (2009).
- [20] G. Mourou and S. Williamson, Appl Phys Lett **41**, 44 (1982).
- [21] V. Ayzvazyan *et al.*, Phys. Rev. Lett. **88**, 104802 (2002).
- [22] I. Grguraš *et al.*, Nat Photonics **6**, 852 (2012).
- [23] W. E. King *et al.*, J Appl Phys **97**, 111101 (2005).
- [24] A. A. Ischenko *et al.*, Physics-Uspekhi **57**, 633 (2014).
- [25] S. A. Aseyev *et al.*, Crystals (Basel) **10**, (2020).
- [26] M. Krüger, M. Schenk, and P. Hommelhoff, Nature **475**, 78 (2011).
- [27] P. Dienstbier *et al.*, Nature **616**, 702 (2023).
- [28] A. Wang *et al.*, Adv. Mater. **35**, 2300185 (2023).
- [29] Y.-J. Kim *et al.*, J Chem Phys **159**, 50901 (2023).

- [30] I. Madan *et al.*, Appl Phys Lett **116**, 230502 (2020).
- [31] C. W. Johnson *et al.*, Phys. Rev. Lett. **129**, 244802 (2022).
- [32] C. W. Johnson *et al.*, Phys. Rev. Appl. **19**, 34036 (2023).
- [33] Y. Pan, B. Zhang, and D. Podolsky, (2023).
- [34] M. Eldar *et al.*, (2023).
- [35] A. Karnieli and S. Fan, Sci Adv **9**, eadh2425 (2023).
- [36] H.-I. Yoo and J. H. Eberly, Phys Rep **118**, 239 (1985).
- [37] S.-Q. Shen, *Topological Insulators* (Springer, 2012).
- [38] J. Goldstone and F. Wilczek, Phys. Rev. Lett. **47**, 986 (1981).
- [39] T. Vachaspati, *Kinks and Domain Walls: An Introduction to Classical and Quantum Solitons* (Cambridge University Press, 2006).
- [40] A. Gover *et al.*, Nat. Phys. **8**, 877 (2012).
- [41] Y. Ji *et al.*, Nature **422**, 415 (2003).
- [42] I. Neder *et al.*, Phys. Rev. Lett. **96**, 16804 (2006).
- [43] M. Kuwahara *et al.*, J Phys Conf Ser **298**, 12016 (2011).
- [44] R. Dahan *et al.*, Science **373**, eabj7128 (2021).
- [45] A. Feist *et al.*, Science **377**, 777 (2022).
- [46] R. Blatt and C. Roos, Nat. Phys. **8**, 277 (2012).
- [47] A. Aspuru-Guzik and P. Walther, Nat. Phys. **8**, 285 (2012).
- [48] I. M. Georgescu, S. Ashhab, and F. Nori, Rev. Mod. Phys. **86**, 153 (2014).
- [49] C. Gross and I. Bloch, Science **357**, 995 (2017).
- [50] A. J. Daley *et al.*, Nature **607**, 667 (2022).
- [51] S. Meier, J. Heimerl, and P. Hommelhoff, Nat. Phys. **19**, 1402 (2023).
- [52] R. Haindl *et al.*, Nat. Phys. **19**, 1410 (2023).

Appendix:

A. Dispersion and chirp of slow electron wavepacket We can express a quantum electron wavefunction in term of a chirped Gaussian wavepacket.

$$\psi_0(z, t) = \frac{e^{i(p_0 z - E_0 t)/\hbar}}{(2\pi\sigma_z^2)^{1/4} \sqrt{1 + i\xi t}} \exp\left(-\frac{(z - v_0 t)^2}{4\sigma_z^2(1 + i\xi t)}\right) \quad (A1)$$

with the free-space chirp factor $\xi = \frac{\hbar}{2m^*\sigma_z^2}$ and the intrinsic wavepacket waist $\sigma_z = \frac{\hbar}{2\sigma_p} = \frac{\hbar v_0}{2\sigma_E}$ and the effective mass $m^* = \gamma^3 m$ with the Lorentz factor γ . Especially for low energy free electron ($\gamma \approx 1$), the second-order dispersion is unavailable. The chirping effect can be expressed in term of the electron width spreading, given by

$$\langle \sigma_z(t) \rangle = \sqrt{\sigma_z^2(1 + \xi^2 t^2)} \quad (A2)$$

For our concern, we choose the kinetic energy of the electron $E_0 = 100 \text{ eV}$ and its group velocity is being $v_0 = \beta c$ with $\beta = 0.02$.

Slow electron experiences stronger dispersion. This is a problem in the development of low energy electron quantum optics. In Bragg regime, only two sidebands are involved, but the sideband has a spectral width. That width actually corresponds to the electron pulse duration with the Heisenberg uncertainty in the quantum limit.

Especially, when the sideband width reaches the energy spacing between two sidebands, we understand that the Bragg regime is not suitable anymore. Indeed, we should consider the spectral spread of each sideband.

B. Derivation of the coupled-mode equations Eq. (1) Here we show the derivation of the coupled-mode equations Eq. (2). Starting from the Hamiltonian Eq. (1), to which we substitute the expression of $A = \frac{E_0}{\omega} \cos[\omega t - qz - \theta(z, t)]$, and neglecting the ponderomotive term (A^2), we obtain $H = \frac{p^2}{2m} - \frac{eE_0}{m\omega} \cos[\omega t - qz - \theta(z, t)] \mathbf{p} - \frac{eE_0 \hbar q}{2im\omega} \sin[\omega t - qz - \theta(z, t)]$. To deal with the problem in the comoving frame, we now define the operator

$$U(t) = e^{-i\frac{\mathbf{p}\omega t}{\hbar q}} \quad (B1)$$

and it follows the identity $U(t)f(z) = e^{-\frac{\omega t}{q}\partial_z}f(z) = f(z - \frac{\omega t}{q})$. Assuming that the solution ψ to our Hamiltonian (1) has the transform $\psi = U(t)\phi = U\phi$, and multiplying the Schrödinger equation, $i\hbar\partial_t\psi = H\psi$, from the left by $U^\dagger = e^{i\frac{p\omega t}{\hbar q}}$, we obtain $i\hbar\partial_t\phi = (U^\dagger H U)\phi - i\hbar[U^\dagger\partial_t U(t)]\phi$, which indicates an effective Hamiltonian for the state ϕ ,

$$H_{\text{eff}} = U^\dagger H U - i\hbar[U^\dagger\partial_t U(t)] \quad (\text{B2})$$

Direct calculation of each term in the right-hand side yields

$$H_{\text{eff}} = \frac{p^2}{2m} - \frac{\omega}{q}\mathbf{p} - \frac{eE_0}{m\omega}\cos(qz + \theta)\mathbf{p} + \frac{eE_0\hbar q}{2im\omega}\sin(qz + \theta) \quad (\text{B3})$$

Transformed into the momentum representation, using the basis of momentum eigenstate $|k\rangle$ ($p = \hbar k$), and the position operator in momentum space $z = i\hbar\partial_p$, we find

$$H_{\text{eff}}|k\rangle = \left[\frac{\hbar^2 k^2}{2m} - \frac{\omega}{q}(\hbar k) \right] |k\rangle - e^{i\theta} \left(\frac{eE_0\hbar k}{2m\omega} + \frac{eE_0\hbar q}{4m\omega} \right) |k - q\rangle - e^{-i\theta} \left(\frac{eE_0\hbar k}{2m\omega} - \frac{eE_0\hbar q}{4m\omega} \right) |k + q\rangle \quad (\text{B4})$$

Here we use $\cos(qz + \theta) = [e^{i(qz + \theta)} + e^{-i(qz + \theta)}]/2$, $\sin(qz + \theta) = [e^{i(qz + \theta)} - e^{-i(qz + \theta)}]/2i$. For our concern, $|k| \gg q$, we can neglect the detuning term $\frac{eE_0\hbar q}{4m\omega}$ in the couplings, and then obtain an effective coupled-mode equations,

$$i\hbar\partial_t|k\rangle = \left(\frac{\hbar^2 k^2}{2m} - \hbar\omega\frac{k}{q} \right) |k\rangle - \kappa|k - q\rangle - \kappa^*|k + q\rangle \quad (\text{B5})$$

with $\kappa = \frac{eE_0\hbar k}{2m\omega}e^{i\theta(z,t)}$, depending on the amplitude strength E_0 . Since the momentum k is a continuous number, we set $k = k_0 + \delta k$, and expand the on-site potential term of Eq. (6), then it becomes $\frac{\hbar^2(k_0 + \delta k)^2}{2m} - \hbar\omega\frac{k_0 + \delta k}{q} = \left(\frac{\hbar^2 k_0^2}{2m} - \hbar\omega\frac{k_0}{q} \right) + \left(\frac{\hbar k_0}{m} - \frac{\omega}{q} \right) \hbar\delta k + \frac{\hbar^2 \delta k^2}{2m}$. We apply the synchronization condition $\frac{\hbar k_0}{m} - \frac{\omega}{q} = 0$, corresponding to $v_g^{(e)} = v_p^{(\text{ph})}$ (the group velocity of electrons equals to the phase velocity of light beam). This condition can locate the central momentum of the electron $p_0 = m\omega/q$, and the energy $E_0 = \frac{p_0^2}{2m} = \frac{m\omega^2}{2q^2}$ (in our setting

$E_0 \sim 100$ eV). Under the synchronization condition, the coupled-mode equations (B5) are simplified as

$$i\hbar \partial_t |\delta k\rangle = \left(\frac{\hbar^2 \delta k^2}{2m} - \frac{\hbar^2 k_0^2}{2m} \right) |\delta k\rangle - \kappa |\delta k - q\rangle - \kappa^* |\delta k + q\rangle \quad (\text{B6})$$

from which one can obtain Eq. (2) in the main text, through shifting $\delta k \rightarrow \delta k \pm q/2$, and absorbing the constant on-site term $\frac{\hbar^2}{2m} \left(\frac{q^2}{4} - k_0^2 \right)$ into the phase of the final solution.

Supplementary information for
“half-electron ($e/2$)” - free electron fractional charge induced by
twisted light

Yiming Pan^{1*}, Ruoyu Yin^{2*}, Yongcheng Ding³, Daniel Podolsky⁴, Bin Zhang^{1,5}

1. School of Physical Science and Technology and Center for Transformative Science,
ShanghaiTech University, Shanghai 200031, China

2. Department of Physics, Institute of Nanotechnology and Advanced Materials,
Bar-Ilan University, Ramat-Gan 52900, Israel

3. International Center of Quantum Artificial Intelligence for Science and Technology (QuArtist) and
Department of Physics, Shanghai University, Shanghai 200444, China

4. Department of Physics, Technion, Haifa 3200003, Israel

5. Department of Electrical Engineering Physical Electronics,
Tel Aviv University, Ramat Aviv 6997801, Israel

1. The full phase-space profiles of the half electron

In our simulations, we consider an electron with center energy 100 eV, corresponding to the group velocity of $v_0 = \beta c$ with the relative speed $\beta = 0.02$ and the Lorentz factor $\gamma = 1.001$. The electron is characterized by a Gaussian wave packet in the momentum space. To achieve synchronization between the phase velocity of light (of wavelength 200 nm) and the group velocity of the electron, we employ a nanograting with a period $\Lambda = 4$ nm.

Conducting a simulation based on the time-dependent Schrödinger equation, as elaborated below, the electron interacts with the light field over a time duration of 6 ps (divided into steps). By directly recording the amplitude of the wave function at each time step, we obtain the temporal profile of the half-electron's spatial distribution. Subsequently, performing a Fourier transform on the recorded wave function to recover the momentum representation, we derive the temporal profile of the half-electron's momentum distribution.

Below we show extended figures, as supplemental materials to Fig. 3 in the main text. We see the initial two sidebands in the momentum space, become smaller in amplitudes and merge with each other, as time elapses, leading to the appearance of more sidebands. And the spatial wave function, exhibits clearly solitary feature, which is manifested by the dispersion-free fact, as time goes by.

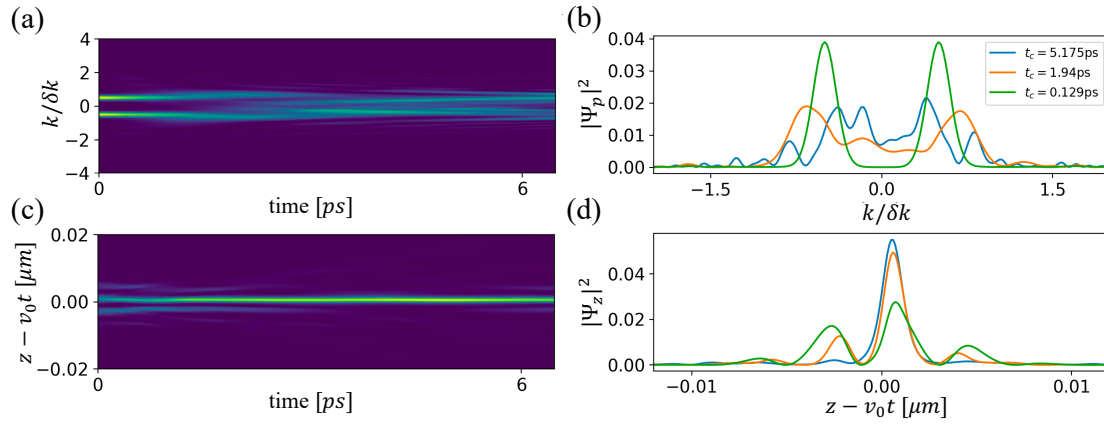


Fig. S1: TDSE simulation of the temporal profile of “half-electron ($e/2$)” by a twisted light wavefront, in both momentum (a,b) and spatial space (c,d). The right column displays snapshots corresponding to the left column, emphasizing the solitary characteristic of the light-induced “half-electron.” Over time, the spatiotemporal profile becomes increasingly distinct, showcasing a pronounced dispersion-free property.

2. TDSE simulation algorithm

In order to assess our tight-binding-approximated result of a two-level electron in the Bragg regime, we have to solve the time-dependent Schrödinger equation (TDSE) directly

$$i\hbar \frac{\partial}{\partial t} \psi(z, t) = \hat{H} \psi(z, t) = (\hat{H}_0 + \hat{H}_I) \psi(z, t), \quad (S2)$$

where the kinetic Hamiltonian of free electron is $\hat{H}_0 = E_0 + v_0(\hat{p} - p_0) + \frac{(\hat{p} - p_0)^2}{2\gamma^3 m_e}$. We choose the initial kinetic energy $\varepsilon_0 = 100 \text{ eV}$, corresponding to the electron velocity $v_0 = \beta c$ with the relative speed $\beta = 0.02$ and the Lorentz factor $\gamma = 1.001$. We take a realistic nanograting, whose longitudinal vector potential is $A(z, t) = -\frac{E_z}{\omega_L} \sin(\omega_L t - k_z z + \theta(z, t))$, with electric field strength E_z , laser frequency ω_L , wavevector $k_z = \frac{2\pi}{\Lambda}$ for a grating with a period Λ , and the phase θ . Thus, the interaction Hamiltonian can be written as

$$\begin{aligned} \hat{H}_I &= -\frac{e}{2\gamma m_e} [\hat{p} \cdot A(z, t) + A(z, t) \cdot \hat{p}] \\ &= -\frac{e}{\gamma m_e} A(z, t) \cdot \hat{p} - i\hbar k_z A_0 \cos(\omega_L t - k_z z + \theta(z, t)) \\ &\simeq -\frac{eA_0}{\gamma m} \sin(\omega_L t - k_z z + \theta(z, t)) \cdot \hat{p} \end{aligned} \quad (S3)$$

where we disregard the second term under the approximation $p_0 \gg \hbar k_z$ (this will be demonstrated in the following), and $\theta(z, t) = -\frac{\pi}{2} \tanh\left(\frac{z - vt - z_0}{0.001}\right)$.

We express the electron wavefunction as the slow-moving part with an initial phase:

$$\psi(z, t) = \chi(z, t) e^{-\frac{i(E_0 t - p_0 z)}{\hbar}} \quad (S4)$$

Thus, the left-hand side (LHS) of Eq. (S2) is

$$i\hbar \frac{\partial}{\partial t} \psi(z, t) = e^{-\frac{i(E_0 t - p_0 z)}{\hbar}} \left(E_0 + i\hbar \frac{\partial}{\partial t} \right) \chi(z, t) \quad (S5)$$

Meanwhile, the right-hand side (RHS) becomes

$$\begin{aligned}
& \left[e^{-\frac{i(E_0 t - p_0 z)t}{\hbar}} \left(E_0 + v_0((\hat{p} + p_0) - p_0) + \frac{((\hat{p} + p_0) - p_0)^2}{2\gamma^3 m_e} \right) \right. \\
& \quad \left. - e^{-\frac{i(E_0 t - p_0 z)t}{\hbar}} \frac{eA_0}{\gamma m_e} \sin(\omega_L t - k_z z + \phi_0) \cdot (\hat{p} + p_0) \right] \chi(z, t) \\
& \quad - \left[e^{-\frac{i(E_0 t - p_0 z)t}{\hbar}} i\hbar k_z \frac{eA_0}{2\gamma m_e} \cos(\omega_L t - k_z z + \phi_0) \right] \chi(z, t) \\
& \simeq e^{-\frac{i(E_0 t - p_0 z)t}{\hbar}} \left(E_0 + v_0 \hat{p} + \frac{\hat{p}^2}{2\gamma^3 m_e} - \frac{eA_0}{\gamma m_e} \sin(\omega_L t - k_z z + \theta(z, t)) \cdot (\hat{p} + p_0) \right) \chi(z, t)
\end{aligned} \tag{S6}$$

here we omit the third term since $\frac{i\hbar k_z}{2} \cos(\omega_L t - k_z z + \phi_0) \ll p_0 \sin(\omega_L t - k_z z + \phi_0)$ under $p_0 \gg \hbar k_z$. Thus, we simplify the TDSE as

$$\begin{aligned}
i\hbar \frac{\partial}{\partial t} \chi(z, t) &= \left(\frac{\hat{p}^2}{2\gamma^3 m} + \left[v_0 - \frac{eA_0}{\gamma m} \sin(\omega_L t - k_z z + \theta(z, t)) \right] \hat{p} \right) \chi(z, t) \\
&\quad - \frac{eA_0 p_0}{\gamma m} \sin(\omega_L t - k_z z + \theta(z, t)) \chi(z, t)
\end{aligned} \tag{S7}$$

Substitute the momentum operator $\hat{p} = -i\hbar \frac{\partial}{\partial z}$ and $p_0 = \gamma\beta mc$, $A_0 = \frac{E_0}{\omega_L}$ yields

$$\begin{aligned}
i\hbar \frac{\partial}{\partial t} \chi(z, t) &= \left(-i\hbar \left[v_0 - \frac{eE_0}{\gamma m \omega_L} \sin(\omega_L t - k_z z + \theta(z, t)) \right] \frac{\partial}{\partial z} \right) \chi(z, t) \\
&\quad - \left[\frac{\hbar^2}{2\gamma^3 m} \frac{\partial^2}{\partial z^2} + \frac{eE_0 \beta c}{\omega_L} \sin(\omega_L t - k_z z + \theta(z, t)) \right] \chi(z, t)
\end{aligned} \tag{S8}$$

The partial difference equation would be solved easier in the co-moving frame:

$$\begin{aligned}
\zeta &= z - v_0 t \\
t' &= t
\end{aligned}$$

and we have

$$\begin{aligned}
d\zeta &= dz - v_0 dt & dz &= d\zeta + v_0 dt' \\
dt' &= dt & dt &= dt'
\end{aligned}$$

which leads to the relations

$$\begin{aligned}
\frac{\partial}{\partial z} &= \frac{\partial}{\partial \zeta} \frac{\partial \zeta}{\partial z} + \frac{\partial}{\partial t'} \frac{\partial t'}{\partial z} = \frac{\partial}{\partial \zeta} \\
\frac{\partial}{\partial t} &= \frac{\partial}{\partial \zeta} \frac{\partial \zeta}{\partial t} + \frac{\partial}{\partial t'} \frac{\partial t'}{\partial t} = \frac{\partial}{\partial t'} - v_0 \frac{\partial}{\partial \zeta}
\end{aligned}$$

In the co-moving frame, Eq. (S8) becomes

$$\begin{aligned} i\hbar \frac{\partial}{\partial t} \psi(z, t) &= i\hbar \left(\frac{\partial}{\partial t'} - v_0 \frac{\partial}{\partial \zeta} \right) \psi(\zeta, \tau_c) \\ &= \left(-i\hbar \left[v_0 + \frac{eE_0}{\gamma m \omega_L} \sin(k_z \zeta - \theta(\zeta)) \right] \frac{\partial}{\partial \zeta} \right) \chi(\zeta, \tau_c) \\ &\quad - \left[\frac{\hbar^2}{2\gamma^3 m} \frac{\partial^2}{\partial \zeta^2} - \frac{eE_0 \beta c}{\omega_L} \sin(k_z \zeta - \theta(\zeta)) \right] \chi(\zeta, \tau_c) \end{aligned}$$

where $\theta(\zeta) = -\frac{\pi}{2} \tanh\left(\frac{\zeta - z_0}{0.001}\right)$ and $\tau_c = ct'$. Divided by $\hbar c$ in both sides, we obtain

$$\begin{aligned} i \frac{\partial}{\partial \tau_c} \chi(\zeta, \tau_c) &= -i \left[\frac{eE_0}{\gamma m c \omega_L} \sin(k_z \zeta - \theta(\zeta)) \right] \frac{\partial}{\partial \zeta} \chi(\zeta, \tau_c) \\ &\quad - \left[\frac{\hbar}{2\gamma^3 m c} \frac{\partial^2}{\partial \zeta^2} - \frac{eE_0 \beta}{\hbar \omega_L} \sin(k_z \zeta - \theta(\zeta)) \right] \chi(\zeta, \tau_c) \end{aligned} \quad (S9)$$

Notice that all the variables are calculated in the length unit of μm and the time of fs . Assume that the electric field on the grating surface is $0.5 \times 10^7 V/m$ and the incident laser $\lambda_L = 0.2 \mu m$. Define

$$\begin{aligned} \alpha_1 &= \frac{eE_0}{\gamma m_e c \omega_L} = 3.11 \times 10^{-7}, \quad \alpha_2 = \frac{\hbar}{2\gamma^3 m_e c} = 1.92 \times 10^{-7} \mu m, \\ \alpha_0 &= \frac{eE_0 \beta}{\hbar \omega_L} = 0.016 \mu m^{-1} \end{aligned}$$

The difference between the Bragg regime and Raman-Nath regime is determined by the factor

$$Q = \frac{\epsilon}{2|\kappa|} = \frac{\alpha_2 k_z^2}{\alpha_0} = \left(\frac{\hbar^2}{2m_e e c^3} \right) \frac{\omega_L^3}{\beta^3 \gamma^3 E_0}$$

For our concern, we choose the parameters $Q = 29.3$ to obtain a two-level electron Rabi oscillation. As a result, the simplified equation is

$$\begin{aligned} i \frac{\partial}{\partial \tau_c} \chi(\zeta, \tau_c) &= -i \left[\beta - \alpha_1 \sin(k_z \zeta - \theta(\zeta)) \right] \frac{\partial}{\partial \zeta} \chi(\zeta, \tau_c) \\ &\quad - \left[\alpha_2 \frac{\partial^2}{\partial \zeta^2} + \alpha_0 \sin(k_z \zeta - \theta(\zeta)) \right] \chi(\zeta, \tau_c) \end{aligned} \quad (S10)$$

Then we apply the discretization for the spatial parameter ζ by dividing the spatial domain into N_ζ parts, with the interval $\delta\zeta = (\zeta_{max} - \zeta_{min})/N_\zeta$, which leads to the following,

$$\begin{aligned}
\frac{\partial^2}{\partial \zeta^2} \chi(\zeta, t) &= \frac{1}{\delta \zeta^2} [\chi(\zeta + \delta \zeta, t) + \chi(\zeta - \delta \zeta, t) - 2\chi(\zeta, t)] \\
-i\beta \frac{\partial}{\partial \zeta} \chi(\zeta, t) &= -\frac{i\beta}{2\delta \zeta} [\chi(\zeta + \delta \zeta, t) - \chi(\zeta - \delta \zeta, t)] \\
i\alpha_1 \sin(k_z \zeta + \theta(\zeta)) \frac{\partial}{\partial \zeta} \chi(\zeta, t) &= -\frac{\alpha_1}{\delta \zeta} \cos(k_z \zeta + \theta(\zeta)) \chi(\zeta, t) \\
&+ \frac{\alpha_1}{2\delta \zeta} [e^{i(k_z \zeta + \theta(\zeta))} \chi(\zeta + \delta \zeta, t) + e^{-i(k_z \zeta + \theta(\zeta))} \chi(\zeta - \delta \zeta, t)]
\end{aligned} \tag{S11}$$

Thus, the discretized Hamiltonian becomes

$$\begin{aligned}
i \frac{\partial}{\partial \tau_c} \chi(\zeta, \tau_c) &= \left[-\frac{\alpha_2}{\delta \zeta^2} - \frac{i\beta}{2\delta \zeta} + \frac{\alpha_1}{2\delta \zeta} e^{i(k_z \zeta + \theta(\zeta))} \right] \chi(\zeta + \delta \zeta, \tau_c) \\
&+ \left[-\frac{\alpha_2}{\delta \zeta^2} + \frac{i\beta}{2\delta \zeta} + \frac{\alpha_1}{2\delta \zeta} e^{-i(k_z \zeta + \theta(\zeta))} \right] \chi(\zeta - \delta \zeta, \tau_c) \\
&+ \left[\frac{2\alpha_2}{\delta \zeta^2} - \frac{\alpha_1}{\delta \zeta} \cos(k_z \zeta + \theta(\zeta)) - \alpha_0 \sin(k_z \zeta + \theta(\zeta)) \right] \chi(\zeta, \tau_c)
\end{aligned} \tag{S12}$$

In order to compute the time evolution of the slow-varying part $\chi(\zeta, \tau_c)$ for a given initial state $\chi(\zeta, \tau_0)$, we define the vector wavefunction with N_ζ components

$$v(\tau) = \left(\chi(\zeta_1, \tau), \chi(\zeta_2, \tau), \dots, \chi(\zeta_{N_\zeta}, \tau) \right)^T \tag{S13}$$

Then, the differential equation (S12) can be simplified as

$$i \frac{\partial}{\partial \tau} v(\tau) = H(\tau) v(\tau) \tag{S14}$$

Applying the time discretization for the interval $\tau - \tau_0$ by equally dividing it into N_t parts with the subinterval $\Delta \tau = (\tau - \tau_0)/N_t$ and we use an implicit Crank-Nicholson integrator to propagate the vector wavefunction from one time step to the next. The formal solution to Eq. (S14) can be expressed in terms of the time evolution operator

$$v(\tau + \Delta \tau) = U(\tau + \Delta \tau, \tau) v(\tau) \tag{S15}$$

where the time evolution operator can be expressed as

$$U(\tau + \Delta \tau, \tau) = (1 + i \Delta \tau H(\tau)/2)^{-1} (1 - i \Delta \tau H(\tau)/2) \tag{S16}$$

The solution of Eq. (S13) can give us the dynamics of the PINEM electron with an initial condition. The final wavefunction could be expressed as

$$v(\tau) = \prod_{n=1}^{N_t} U(\tau_0 + n\Delta\tau, \tau_0 + (n-1)\Delta\tau) v(\tau_0) \quad (S17)$$